

Interaction between monolayer graphene and terahertz resonant metamaterials

Shuyuan Xiao¹, Tao Wang¹, Xiaoyun Jiang¹, Xicheng Yan¹, Le Cheng¹, Boyun Wang² and Chen Xu³

¹ Wuhan National Laboratory for Optoelectronics, Huazhong University of Science and Technology, Wuhan 430074, People's Republic of China

² School of Physics and Electronic-information Engineering, Hubei Engineering University, Xiaogan 432000, People's Republic of China

³ Department of Physics, New Mexico State University, Las Cruces 88001, United State of America

E-mail: wangtao@hust.edu.cn

February 2017

Abstract. Graphene has emerged as a promising building block in the modern optics and optoelectronics due to its novel optical and electrical properties. The semi-metallic behavior and the electrical tunability are combined to achieve tunable surface plasmon resonances (SPRs) and give rise to a range of active applications. However, the interaction between graphene and metal-based resonant metamaterials, known as the passive response, has not been fully understood. In this work, a comparative investigation on the interaction between the monolayer and the terahertz (THz) resonances supported by the asymmetric split ring (ASR) metamaterials is systematically conducted. The simulation results show that the monolayer graphene can substantially reduce Fano resonance and even switch it off, while leave the dipole resonance nearly unaffected, which phenomenon is well explained with the high conductivity of graphene. The different behaviors of the two resonance modes can be important in designing active metal-graphene hybrid metamaterials. In addition, the "sensitivity" to the monolayer graphene of Fano resonance is also highly appreciated in the field of ultrasensitive sensing, where the novel physical mechanism can be employed in sensing other graphene-like two-dimensional (2D) materials or biomolecules with the high conductivity.

1. Introduction

Graphene, a monolayer of carbon atoms arranged in plane with a honeycomb lattice, is a two-dimensional (2D) material. Since the first report of its synthesis via a "Scotch tape" method in 2004, graphene has emerged as a popular research topic in the fields of optics and optoelectronics[1, 2, 3]. Among its many novel properties, the semi-metallic behavior is one of the most fascinating ones, and based on which, graphene can couple to the incidence light and support surface plasmon resonances (SPRs)

in the mid-infrared and terahertz (THz) regime[4, 5, 6]. The propagating SPRs in graphene waveguides make it possible to guide light with deep subwavelength mode profiles[7, 8, 9], and in the meanwhile, the localized SPRs in graphene metamaterials lead to efficient light confinement and strong near-field enhancement[10, 11]. Moreover, the continuously tunable optical conductivity of graphene via manipulating its Fermi energy enables active SPRs[12, 13], offering much more flexibility than traditional plasmonic materials, thus give rise to a range of active applications such as absorbers[14, 15, 16], biosensors[17, 18], filters[19, 20], modulators[21, 22] and photodetectors[23, 24, 25]. Though the function role of graphene in the active control of SPRs has been extensively investigated, the interaction between graphene and metal-based resonant micro/nanostructures, known as the passive response, has not been fully understood. Technically, the passive response is equally important since it may provide new opportunities to reveal novel physical mechanisms as well as feed back precursors for the calibration of active control and application development of metal-graphene hybrid micro/nanostructures[26, 27, 28].

To this end, a simulation investigation on the interaction between the monolayer graphene and metal-based resonant metamaterials is systematically conducted in this work. The classical THz metamaterials composed of an array of asymmetric split rings (ASRs) is employed here to simultaneously support both the dipole resonance and Fano resonance. The simulation results show that the presence of the monolayer graphene on the top of ASR metamaterials can substantially reduce Fano resonance and even switch it off, while leave the dipole resonance nearly unaffected. The different behaviors of the two resonance modes together with the underlying physical mechanism can be important in designing active metal-graphene hybrid metamaterials. In addition, considering the ultra thin thickness of the monolayer graphene (~ 1 nm), the "sensitivity" of Fano resonance here is also highly appreciated in the field of ultrasensitive sensing, where the novel physical mechanism can be employed in sensing other graphene-like 2D materials or biomolecules.

2. The geometric structure and numerical model

The schematic geometry of our proposed structure is depicted in Figure 1. The unit cell is arranged in a period array with a lattice constant $P = 60$ μm and composed of a two-gap aluminum split ring on the top of a silicon substrate. The radius, the width and the thickness of the resonator are respectively $R = 21$ μm , $W = 6$ μm and $t_{Al} = 200$ nm, and the substrate is assumed to be semi-infinite. The central angles of the lower and the upper arcs of the two-gap split ring are denoted by θ_1 and θ_2 . The optical constants of aluminum in the THz regime are described by a Drude model $\varepsilon_{Al} = \varepsilon_\infty - \omega_p^2/(\omega^2 + i\omega\gamma)$ with the plasmon frequency $\omega_p = 2.24 \times 10^{16}$ rad/s and the damping constant $\gamma = 1.22 \times 10^{14}$ rad/s[29]. The refractive index of the silicon is taken as $n_{Si} = 3.42$.

The monolayer graphene is placed on the top of the two-gap split ring metamaterials

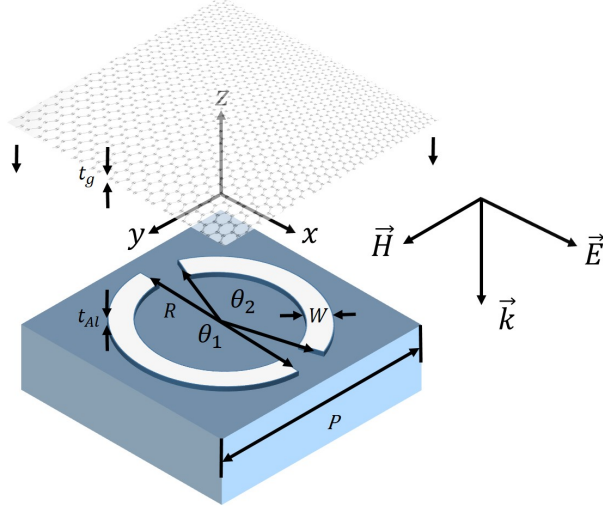


Figure 1: The schematic geometry of our proposed structure.

and modeled as a 2D plane with the effective thickness $t_g = 1$ nm. The surface conductivity of graphene in the THz regime is dominated by the intraband transport processes and also treated according to a Drude-like model $\sigma_g = iD/[\pi(\omega + i\Gamma)]$ with the Drude weight $D = 1 \times 10^3 \times G_0$ cm $^{-1}$ and the carrier scattering rate $\Gamma = 110$ cm $^{-1}$ as fitting parameters, where $G_0 = 2e^2/h$ is the quantum of conductance[30, 31]. The complex permittivity of graphene can thus be calculated by $\varepsilon_{g,r} = -\sigma_{g,i}/(\omega t_g \varepsilon_0)$ and $\varepsilon_{g,i} = \sigma_{g,r}/(\omega t_g \varepsilon_0)$, where $\sigma_{g,r}$ and $\sigma_{g,i}$ are the real and imaginary part of complex conductivity of graphene, and ε_0 is the permittivity of vacuum[32].

As previously reported, the two-gap split ring metamaterials can simultaneously support both a bright dipole resonance and a dark Fano resonance if the symmetry of the structure is broken[33, 34], which can provide an excellent platform for the comparative investigation on the interaction between the monolayer graphene and THz resonances. In the initial setup, the central angles of the lower and the upper arcs of the two-gap split ring are equally set to $\theta_1 = \theta_2 = 160^\circ$ to form symmetric split ring (SRR) metamaterials. The asymmetry is gently introduced with the increase of θ_1 and the decrease of θ_2 to make ASR metamaterials, and the asymmetry degree is defined as $\Delta\theta = \theta_1 - \theta_2$. The influence of the monolayer graphene on the THz resonances with different $\Delta\theta$ will be analyzed to reveal the novel physical mechanism behind it using the finite-difference time-domain (FDTD) method. The periodical boundary conditions are employed in the x and y directions and perfectly matched layers are utilized in the z direction along the propagation of the incidence plane wave.

3. Simulation results and discussions

The THz plane wave is illuminated along the negative z -axis with the electric field oriented perpendicular to the gaps. The simulated transmission spectra through the two-gap split ring metamaterials without and with the monolayer graphene is shown in

Figure 2, where the asymmetry degree is varied from 0° to 40° .

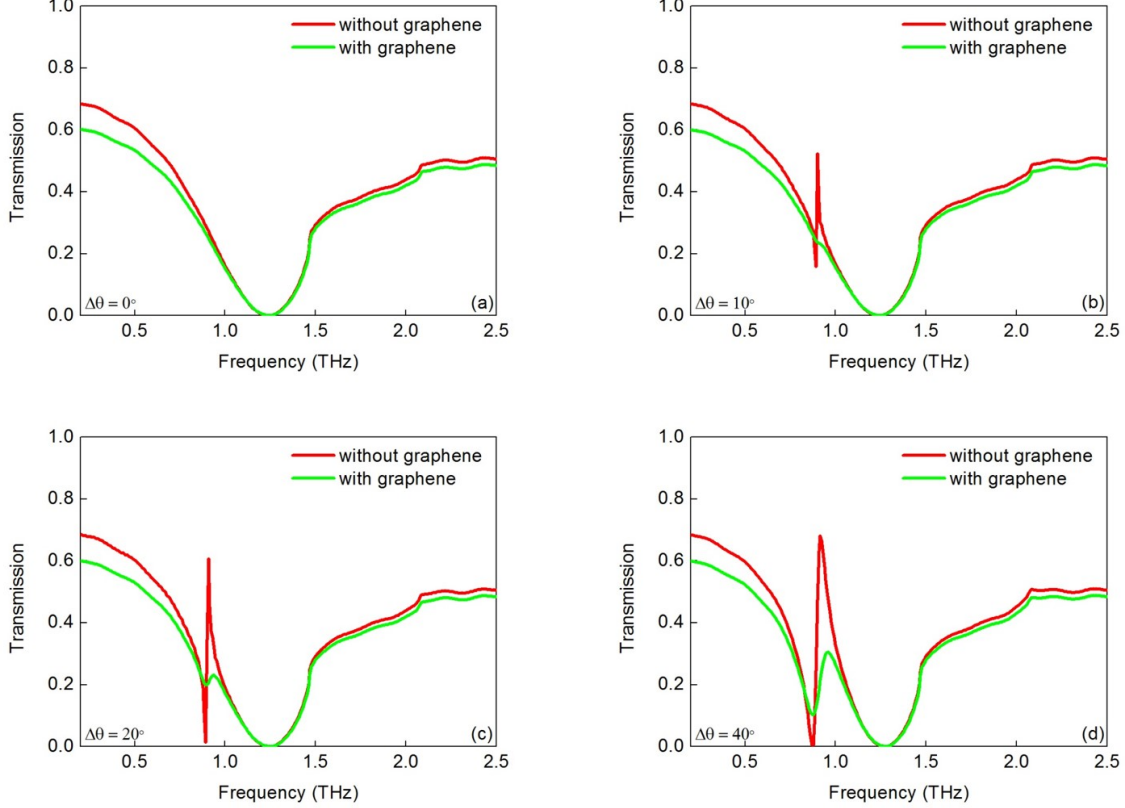


Figure 2: The simulated transmission spectra through the two-gap split ring metamaterials without and with the monolayer graphene. The asymmetry degree is varied from 0° to 40° , as shown in the insets.

In the absence of the monolayer graphene, with the asymmetry degree $\Delta\theta = 0^\circ$, the SSR metamaterials show a symmetric resonance at 1.24 THz, which is known as the bright dipole mode. It is the basic and direct response of metamaterials to the free-space light and exhibits a broad resonance line width caused by the strong radiative losses. When a slight asymmetry $\Delta\theta = 10^\circ$ is introduced, SSR metamaterials turn into ASR ones, along with two resonances appearing in the transmission spectrum, one which is identical to that of SSR metamaterials and recognized as the dipole mode, the other is an asymmetric Fano resonance located at 0.89 THz. This additional ultra sharp resonance results from a subradiative dark mode where the radiative losses are near completely suppressed and the line width of the transmission profile is solely limited by the intrinsic metal losses (Drude damping)[35]. With the increase of the asymmetry degree, the dipole resonance has little change except the resonance frequency shifting to 1.27 THz, which once again demonstrate the fundamentality of this bright mode in the symmetric as well as the asymmetric metamaterials, and in the meanwhile, Fano resonances remain at the nearly fixed frequency and become even more pronounced,

where the steeper dips can be nicely observed in the respective spectra with $\Delta\theta = 20^\circ$ and $\Delta\theta = 40^\circ$.

In the presence of the monolayer graphene, the profile of the broad dipole resonance is pretty much the same as that in the previous case with every asymmetry degree, which indicates that the bright mode does not interact with the monolayer graphene. By contrast, however, Fano resonance experiences a great change. Though the trend of the increase in the amplitude of Fano resonance is retained with the increase of asymmetry degree, the absolute strength is substantially reduced and even switched off. In order to characterize the induced change in the resonance strength due to the presence of the monolayer graphene, the reduction degree in the transmission is introduced as $\Delta T = |T_0 - T_g| \times 100\%$, where T_0 and T_g are the transmission amplitudes at the dip of Fano resonance without and with the monolayer graphene. When the asymmetry degree starts at $\Delta\theta = 10^\circ$, the reduction degree in the transmission is $\Delta T_{10} = 8.42\%$. As $\Delta\theta$ increases to 20° , the reduction degree goes up to $\Delta T_{20} = 18.6\%$. Finally when $\Delta\theta$ comes to 40° , the reduction degree gets back to $\Delta T_{40} = 9.67\%$. In comparison with that on the dipole resonance, the monolayer graphene has a much more pronounced effect on Fano resonance, which implies the existence of a strong interaction between the monolayer graphene and ASR metamaterials at Fano frequency.

To reveal the physical mechanism behind the novel phenomenon, the essences of the dipole and Fano resonances are reviewed. The simulated electric field distributions at the dipole resonance and Fano resonance without the monolayer graphene are plotted in Figure 3, where the asymmetry degree is $\Delta\theta = 10^\circ$. For the dipole resonance at 1.24 THz, a vertically symmetric distribution of the electric field along the lower and upper arcs of ASR can be nicely observed and the net induced dipoles in the THz metamaterials exhibit a clear tendency to follow the polarization of the incidence plane wave, which lead to the accumulation of the same type of charges at the two gaps. For Fano resonance at 0.89 THz, the electric field enhancement is much more pronounced since the asymmetric mode is only weakly coupled to the free-space light. A circulation distribution of the electric field along the entire ASR makes it a magnetic dipole and can be phenomenologically understood in terms of a *LC*-oscillator with the two gaps serving as effective capacitors, where a large amount of the opposite type of charges are accumulated. By comparison, the different distribution types should be the reason why the two resonances behave differently to the monolayer graphene. The underlying physical mechanism lies in the high conductivity of graphene. Once the monolayer graphene is placed on the top of the THz metamaterials, it connects the lower and upper arcs of ASR, shorten the two gaps and thus influences the charge distributions. For the dipole resonance, the presence of the monolayer graphene does not cause a significant change in the transmission spectrum in that the shorting of the two gaps would not influence the accumulation of the same type of charges. For Fano resonance, however, the opposite type of charges at the ends of the two gaps can be recombined and neutralized through the highly conductive graphene, which leads a strong suppression of the electric field enhancement. Therefore, the absolute strength of Fano resonance

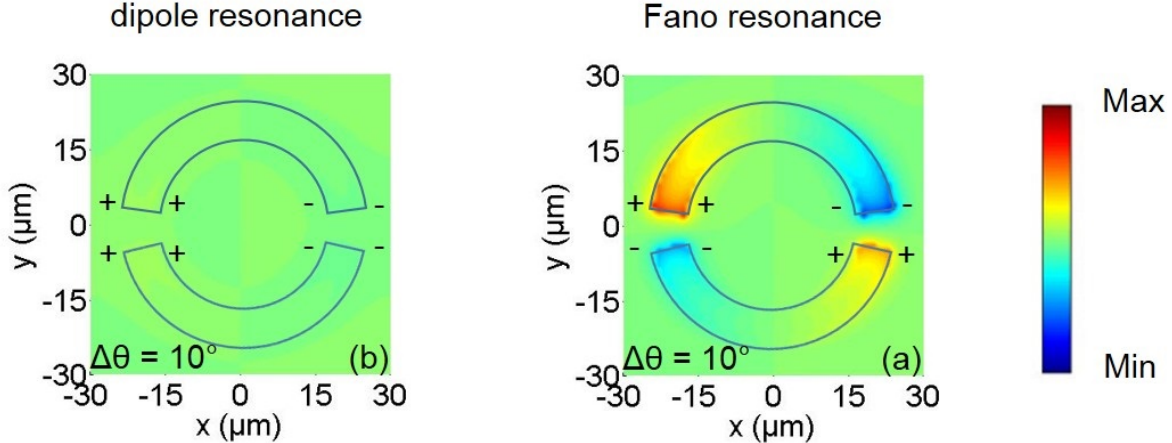


Figure 3: The simulated electric field distributions at the dipole resonance and Fano resonance without the monolayer graphene. The asymmetry degree is 10° , as shown in the insets.

would be substantially reduced and even switched off in the transmission spectrum.

To demonstrate the proposed physical mechanism, the simulated electric field distributions at Fano resonance without and with the monolayer graphene are compared in Figure 4, where the asymmetry degree is varied from 10° to 40° . When the asymmetry degree starts at $\Delta\theta = 10^\circ$, the strong enhancement of the electric field in the gaps is near completely suppressed with the monolayer graphene placed on the top of ASR metamaterials, which corresponds to the switch-off of Fano resonance in the transmission spectrum. With the increase of asymmetry degree to $\Delta\theta = 20^\circ$, the electric field enhancement without the monolayer graphene become even more pronounced, while that with the presence of the monolayer graphene increases only slightly, leading to the larger change in the absolute strength of Fano resonance. Finally when $\Delta\theta = 40^\circ$, the electric field enhancement begins to fall, and in the meanwhile, that with graphene further goes up, which accordingly explains the decrease of the reduction degree in the transmission.

In the real cases, there would be unavoidable disorders generated by the environment during the growth or transfer processes of graphene. The multilayer graphene can be found either in twisted configurations where the layers are rotated relative to each other or graphitic Bernal stacked configurations where half the atoms in one layer lie on half the atoms in others[36]. Previous investigations have claimed the randomly stacked monolayer graphene would still behave as the isolated monolayer graphene owing to the electrical decoupling and the conductivity becomes proportional to the layer number[37, 38]. Considering this, the transmission spectra through the two-gap split ring metamaterials with the bilayer and the trilayer graphene also simulated in Figure 5. As with the monolayer graphene, the dipole resonance still does not interact with the multilayer graphene in that the shorting of the two gaps would not influence the accumulation of the same type of charges. But on the other hand, the presence

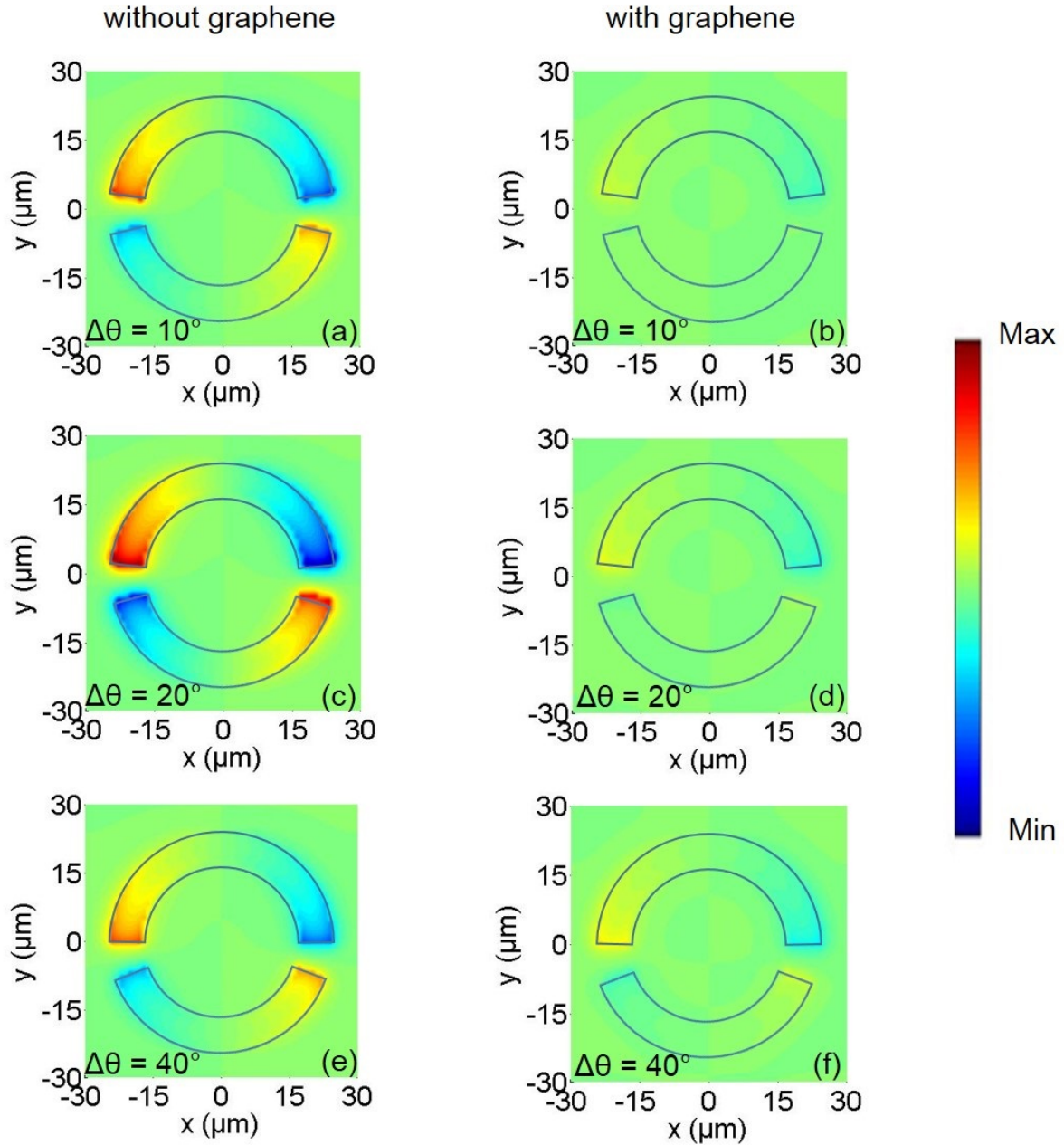


Figure 4: The simulated electric field distributions at Fano resonance without and with the monolayer graphene. The asymmetry degree is varied from 10° to 40° , as shown in the insets.

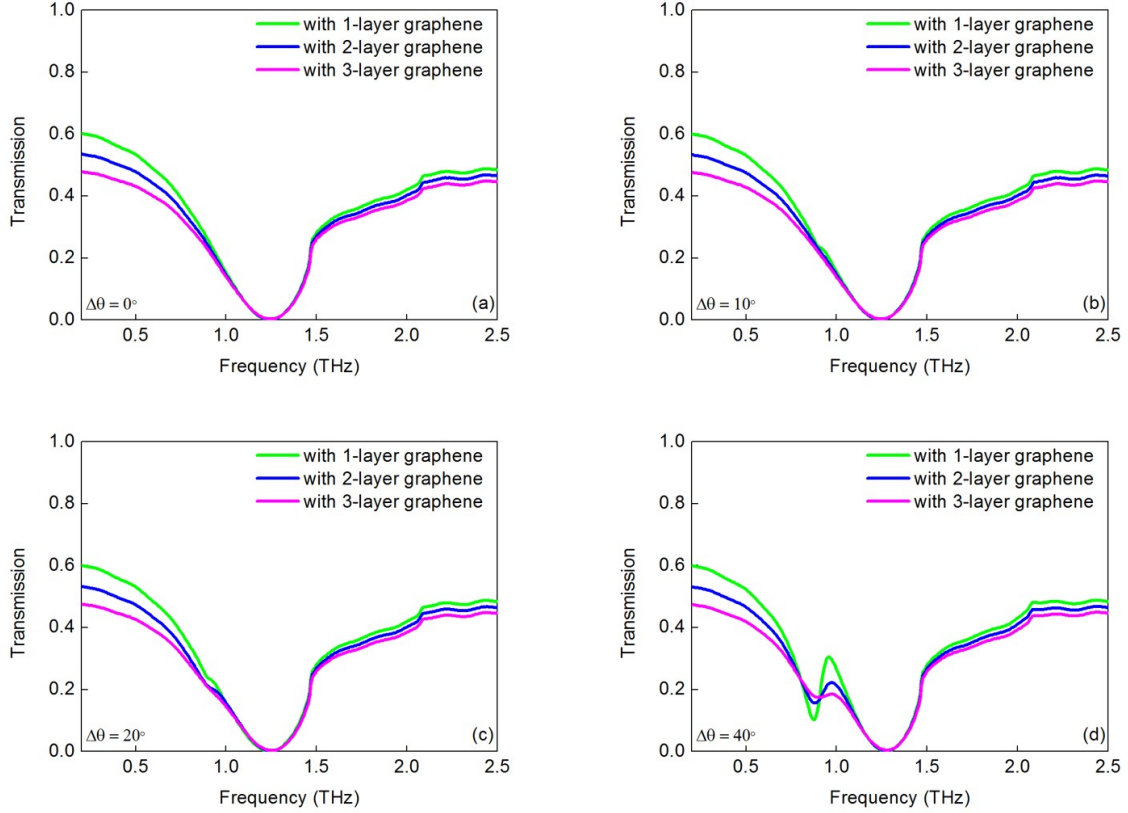


Figure 5: The simulated transmission spectra through the two-gap split ring metamaterials with the multilayer graphene. The asymmetry degree is varied from 0° to 40° , as shown in the insets.

of the multilayer graphene further reduces the absolute strength of Fano resonance in the transmission spectra due to the higher conductivity, where this resonance mode is near completely switched off with $\Delta\theta = 10^\circ$ and $\Delta\theta = 20^\circ$ and the steepest dip with $\Delta\theta = 40^\circ$ become quite moderate. These simulation results are in accordance with the relationship between conductivity and the layer number of graphene and in turn demonstrate our proposed physical mechanism, which is therefore of importance and practical significance to feed back precursors for the calibration of active control and application development of metal-graphene hybrid micro/nanostructures. In addition, the "sensitivity" to the monolayer graphene of Fano resonance in the ASR metamaterials can also be employed in the field of ultrasensitive sensing. In general, sensing with THz metamaterials requires the analyte with a thickness of hundreds of nanometers[39, 40], however, in our case, the ultra thin (~ 1 nm) monolayer graphene is detected, which can be extended to other graphene-like 2D materials or biomolecules with the high conductivity.

4. Conclusions

In conclusions, the interaction between the monolayer graphene and THz resonances is numerically investigated in this work. It is found that the presence of the graphene on the top of ASR metamaterials can substantially reduce Fano resonance and even switch it off, while leave the dipole resonance nearly unaffected. This novel phenomenon is well explained with the high conductivity of graphene, which can recombine and neutralize the opposite type of charges at the ends of the two gaps, and leads a strong suppression of the absolute strength of Fano resonance. The bilayer and trilayer graphene as disorders in the real cases are also included to explore the practical possibility and the results coincide with the monolayer case. Therefore the different behaviors of the two resonance modes together with the underlying physical mechanism are of importance and practical significance in designing active metal-graphene hybrid metamaterials. In addition, the "sensitivity" to the monolayer graphene of Fano resonance in the ASR metamaterials is also highly appreciated in the field of ultrasensitive sensing, where the novel physical mechanism can be employed in sensing other graphene-like 2D materials or biomolecules with the high conductivity.

Acknowledgments

The author Shuyuan Xiao (SYXIAO) expresses his deepest gratitude to his Ph.D. advisor Tao Wang for providing guidance during this project. SYXIAO would also like to thank Dr. Qi Lin and Dr. Guidong Liu (Hunan University) for beneficial discussions on graphene optical properties. This work is supported by the National Natural Science Foundation of China (Grant No. 61376055, 61006045 and 11647122), the Fundamental Research Funds for the Central Universities (HUST: 2016YXMS024) and the Project of Hubei Provincial Department of Education (Grant No. B2016178).

References

- [1] Novoselov K S, Geim A K, Morozov S V, Jiang D, Zhang Y, Dubonos S V, Grigorieva I V and Firsov A A 2004 Electric field effect in atomically thin carbon films *Science* **306** 666-669
- [2] Bonaccorso F, Sun Z, Hasan T and Ferrari A C 2010 Graphene photonics and optoelectronics *Nat. Photonics* **4** 611-622
- [3] de Abajo F J G 2013 Graphene nanophotonics *Science* **339** 917-918
- [4] Grigorenko A N, Polini M and Novoselov K S 2012 Graphene plasmonics *Nat Photonics* **6** 749-758
- [5] Garcia de Abajo F J 2014 Graphene plasmonics: challenges and opportunities *ACS Photonics* **1** 135-152
- [6] He X, Gao P and Shi W 2016 A further comparison of graphene and thin metal layers for plasmonics *Nanoscale* **8** 10388-10397
- [7] Nikitin A Y, Guinea F, Garcia-Vidal F J and Martin-Moreno L 2011 Edge and waveguide terahertz surface plasmon modes in graphene microribbons *Phys Rev B* **84** 161407
- [8] Lin Q, Zhai X, Wang L, Wang B, Liu G and Xia S 2015 Combined theoretical analysis for plasmon-induced transparency in integrated graphene waveguides with direct and indirect couplings *EPL* **111** 34004

[9] Han X, Wang T, Li X, Xiao S and Zhu Y 2015 Dynamically tunable plasmon induced transparency in a graphene-based nanoribbon waveguide coupled with graphene rectangular resonators structure on sapphire substrate *Opt Express* **23** 31945-31955

[10] Zhang J, Zhu Z, Liu W, Yuan X and Qin S 2015 Towards photodetection with high efficiency and tunable spectral selectivity: graphene plasmonics for light trapping and absorption engineering *Nanoscale* **7** 13530-13536

[11] Xiao S, Wang T, Liu Y, Xu C, Han X and Yan X 2016 Tunable light trapping and absorption enhancement with graphene ring arrays *Phys Chem Chem Phys* **18** 26661-26669

[12] Ju L, Geng B, Horng J, Girit C, Martin M, Hao Z, Bechtel H A, Liang X, Zettl A, Shen Y R and Wang F 2011 Graphene plasmonics for tunable terahertz metamaterials *Nat Nanotechnol* **6** 630-634

[13] Hu H, Zhai F, Hu D, Li Z, Bai B, Yang X and Dai Q 2015 Broadly tunable graphene plasmons using an ion-gel top gate with low control voltage *Nanoscale* **7** 19493-19500

[14] Tahersima M H and Sorger V J 2015 Enhanced photon absorption in spiral nanostructured solar cells using layered 2D materials *Nanotechnology* **26** 344005

[15] Wu J 2016 Tunable ultranarrow spectrum selective absorption in a graphene monolayer at terahertz frequency *J Phys D Appl Phys* **49** 215108

[16] Linder J and Halterman K 2016 Graphene-based extremely wide-angle tunable metamaterial absorber *Sci Rep* **6** 31225

[17] Li K, Ma X, Zhang Z, Song J, Xu Y and Song G 2014 Sensitive refractive index sensing with tunable sensing range and good operation angle-polarization-tolerance using graphene concentric ring arrays *J Phys D Appl Phys* **47** 405101

[18] Yan X, Wang T, Han X, Xiao S, Zhu Y and Wang Y 2016 High sensitivity nanoplasmonic sensor based on plasmon-induced transparency in a graphene nanoribbon waveguide coupled with detuned graphene square-nanoring resonators *Plasmonics* doi:10.1007/s11468-016-0405-0

[19] Li H J, Wang L L, Liu J Q, Huang Z R, Sun B and Zhai X 2013 Investigation of the graphene based planar plasmonic filters *Appl Phys Lett* **103** 211104

[20] Li H J, Wang L L, Liu J Q, Huang Z R, Sun B and Zhai X 2014 Tunable, mid-Infrared ultra-narrowband filtering effect induced by two coplanar graphene strips *Plasmonics* **9** 1239-1243

[21] Andersen D R 2010 Graphene-based long-wave infrared TM surface plasmon modulator *JOSA B* **27** 818-823

[22] He X, Li T, Wang L, Wang J, Jiang J, Yang G, Meng F and Wu Q 2014 Electrically tunable terahertz wave modulator based on complementary metamaterial and graphene *J Appl Phys* **115** 17B903

[23] Fang Z, Liu Z, Wang Y, Ajayan P M, Nordlander P and Halas N J 2012 Graphene-antenna sandwich photodetector *Nano Lett* **12** 3808-3813

[24] Freitag M, Low T, Zhu W, Yan H, Xia F and Avouris P 2013 Photocurrent in graphene harnessed by tunable intrinsic plasmons *Nat Commun* **4** 1951

[25] Gowda P, Mohapatra D R and Misra A 2014 Nonlinear optical absorption in a graphene infrared photodetector *Nanotechnology* **25** 335710

[26] Papasimakis N, Luo Z, Shen Z X, de Angelis F, di Fabrizio E, Nikolaenko A E and Zheludev N I 2010 Graphene in a photonic metamaterial *Opt Express* **18** 8353-8359

[27] Dabidian N, Kholmanov I, Khanikaev A B, Tatar K, Trendafilov S, Mousavi S H, Magnuson C, Ruoff R S and Shvets G 2015 Electrical switching of infrared light using graphene integration with plasmonic Fano resonant metasurfaces *ACS Photonics* **2** 216-227

[28] Chakraborty S, Marshall O P, Folland T G, Kim, Y J, Grigorenko A N and Novoselov K S 2016 Gain modulation by graphene plasmons in aperiodic lattice lasers *Science* **351** 246-248

[29] Ordal M A, Bell R J, Alexander R W, Long L L and Querry M R 1985 Optical properties of fourteen metals in the infrared and far infrared: Al, Co, Cu, Au, Fe, Pb, Mo, Ni, Pd, Pt, Ag, Ti, V, and W *Appl Optics* **24** 4493-4499

[30] Yan H, Xia F, Zhu W, Freitag M, Dimitrakopoulos C, Bol A A, Tulevski G and Avouris P 2011

Infrared spectroscopy of wafer-scale graphene *ACS Nano* **5** 9854-9860

- [31] Jnawali G, Rao Y, Yan H and Heinz T F 2013 Observation of a transient decrease in terahertz conductivity of single-layer graphene induced by ultrafast optical excitation *Nano lett* **13** 524-530
- [32] Lee S H, Choi M, Kim T T, Lee S, Liu M, Yin X, Choi H K, Lee S S, Choi C G, Choi S Y, Zhang X and Min B 2012 Switching terahertz waves with gate-controlled active graphene metamaterials *Nat Materials* **11** 936-941
- [33] Singh R, Al-Naib I A I, Koch M and Zhang W 2011 Sharp Fano resonances in THz metamaterials *Opt Express* **19** 6312-6319
- [34] Singh R, Al-Naib I, Cao W, Rockstuhl C, Koch M and Zhang W 2013 The Fano resonance in symmetry broken terahertz metamaterials *IEEE Trans THz Sci Techn* **3** 820-826
- [35] Liu N, Weiss T, Mesch M, Langguth L, Eigenthaler U, Hirscher M, Sonnichsen C and Giessen H 2009 Planar Metamaterial Analogue of Electromagnetically Induced Transparency for Plasmonic Sensing *Nano Lett* **10** 1103-1107
- [36] Brown L, Hovden R, Huang P, Wojcik M, Muller D A and Park J 2012 Twinning and twisting of tri-and bilayer graphene *Nano Lett*, **12** 1609-1615
- [37] Chen H T, Padilla W J, Zide J M O, Gossard A C, Taylor A J and Averitt R D 2006 Active terahertz metamaterial devices *Nature* **444** 597-600
- [38] Hass J, Varchon F, Millan-Otoya J E, Sprinkle M, Sharma N, de Heer W A, Berger C, First P N, Magaud L and Conrad E H 2008 Why Multilayer Graphene on 4H-SiC (0001) Behaves Like a Single Sheet of Graphene *Phys Rev Lett* **100** 125504
- [39] O'Hara J F, Singh R, Brener I, Smirnova E, Han J, Taylor A J and Zhang W 2008 Thin-film sensing with planar terahertz metamaterials: sensitivity and limitations *Opt Express* **16** 1786-1795
- [40] Tao H, Strikwerda A C, Liu M, Mondia J P, Ekmekci E, Fan K, Kaplan D L, Padilla W J, Zhang X, Averitt R D and Omenetto F G 2010 Performance enhancement of terahertz metamaterials on ultrathin substrates for sensing applications *Appl Phys Lett* **97** 261909